Translational Oncology
www.transonc.com

Volume 7 Number 2 April 2014 pp. 188–195 188

The Role of Angiopoietins as Potential Therapeutic Targets in Renal Cell Carcinoma[1]

Xiaoen Wang*,†, Andrea J. Bullock†, Liang Zhang†, Lin Wei†, Dongyin Yu‡, Kedar Mahagaokar†, David C. Alsop*, James W. Mier†, Michael B. Atkins§, Angela Coxon‡, Jon Oliner‡ and Rupal S. Bhatt†

*Department of Radiology, Beth Israel Deaconess Medical Center, Harvard Medical School, Boston, MA; †Division of Hematology-Oncology and Cancer Biology, Beth Israel Deaconess Medical Center, Harvard Medical School, Boston, MA; ‡Oncology Research, Amgen Inc, Thousand Oaks, CA; §Departments of Oncology and Medicine, Georgetown-Lombardi Comprehensive Cancer Center, Washington, DC

Abstract

Angiopoietin 2 (Ang2) is a secreted glycoprotein upregulated at sites of angiogenesis and has been implicated in cancer neovascularization. Recent studies have suggested efficacy of combined Ang and vascular endothelial growth factor receptor (VEGFR) inhibition for patients with metastatic renal cell carcinoma (mRCC). We measured Ang2 expression in human tissue and plasma, and tested the effect of dual Ang1/2 (trebananib; AMG386) or Ang2 alone (L1-7) inhibition with VEGFR inhibition on murine RCC growth and blood flow. Ang2 levels were higher in human tumors than normal tissues with RCC ranking highest for Ang2 expression across all tumor types tested. Plasma Ang2 was significantly higher in patients with mRCC compared to controls or patients with stage I disease. Plasma Ang2 decreased with sunitinib treatment and increased at time of disease progression. In the RCC mouse, dual Ang1/2 and Ang2 inhibition improved the activity of sunitinib. Combined Ang1/2 and VEGFR inhibition prevented the resumption of blood flow associated with sunitinib resistance. Thus, Ang2 inhibition, independent of Ang1 inhibition, improves the activity of sunitinib and plasma Ang2 increases in the setting of progression on sunitinib possibly contributing to resistance. Further, arterial spin-labeled perfusion magnetic resonance imaging might be a non-invasive marker of the antiangiogenic activity of Ang inhibitors.

Translational Oncology (2014) 7, 188–195

Introduction

Vascular endothelial growth factor receptor (VEGFR) inhibition has shown significant antitumor and antiangiogenic activity in patients with renal cell carcinoma (RCC). Agents such as sunitinib, sorafenib, pazopanib, and axitinib have all shown activities in patients with metastatic RCC [1-4] leading to Food and Drug Administration approval. However, antiangiogenic therapy with VEGFR tyrosine kinase inhibitors (TKIs) does not lead to durable or complete responses and treatment resistance develops at a median of 9 to 12 months.

Resistance could be associated with selection of tumor cells that can survive treatment-induced hypoxia or through activation of angiogenic pathways parallel to the VEGF axis. We have shown that resistance to therapy is associated with resumption of angiogenesis despite continued therapy, consistent with the activation of alternate angiogenic pathways [5,6]. Others have implicated angiogenic factors, such as interleukin 8 and fibroblast growth factor in resistance [7,8]. One additional pathway that has recently been the

Address all correspondence to: Rupal S. Bhatt, MD/PhD, Division of Hematology-Oncology and Cancer Biology, Beth Israel Deaconess Medical Center, 330 Brookline Avenue, Boston, MA 02215.

[1] This work was supported by the Dana-Farber/Harvard Cancer Center Kidney Cancer SPORE (Specialized Programs of Research Excellence) (NIH, National Institutes of Health, 2P50CA101942-08), NIH K08 CA138900-03 to R.S.B., and a grant from Amgen.
Received 19 September 2013; Revised 10 December 2013; Accepted 2 January 2014

http://dx.doi.org/10.1016/j.tranon.2014.02.003

Table 1. The List of Primers Used in the Gene Expression Studies by RT-PCR.

	Forward Primer	Reverse Primer	Probe
Ang1	GGA GGA TGG TGG TTT GAT GC	TGG TTT TGT CCC GCA GTA TAG A	<6FAM>TG TGG CCC CTC CAA TCT AAA TGG AAT G<TAM>
Ang2	TAC ACT TTC CTC CTG CCA GAG AT	TGC ACA GCA TTG GAC ACG T	<6FAM>CA ACT GCC GCT CTT CCT CCA GCC <TAM>
CD31	CGG TGC AAA ATG GGA AGA A	TGA CGT GAG AGG TGG TGC TG	<6FAM>TG ACC CTG CAG TGC TTC GCG G<TAM>
VEGFR2	GAC AGA GGG ACT TGG ACT GGC	CTC AGT CAC CTC CAC CCT TTG	<6FAM>TG GCC CAA TAA TCA GAG TGG CAG TGA <TAM>
VEGF	GGG CAG AAT CAT CAC GAA GTG	GGT CTC GAT TGG ATG GCA GT	<6FAM>TG AAG TTC ATG GAT GTC TAT CAG CGC AGC <TAM>

subject of much investigation is the angiopoietin (Ang) axis. Ang2 inhibition has been shown to have activity in preclinical models and several agents are currently being tested in clinical settings across multiple tumor types [9-12]. While much is known about the role of Ang2 in cancer, several important unanswered questions exist. Ang1 and Ang2 are endothelial-secreted proteins with a complex relationship and potentially competing overall effects on tumor angiogenesis. Ang2 is most commonly described as a molecule that destabilizes vascular networks, supporting neoangiogenesis [13,14]. Ang1 binds to the Tie2 receptor to promote vascular maturation, inhibiting angiogenesis. Ang2 is an antagonist of Ang1 signaling through Tie2. Thus, one of the key questions in the Ang field is whether, in RCC, Ang1 inhibition undermines or augments effects of Ang2 inhibition.

In previous studies, the Ang2-specific inhibitor L1-7, Ang2-CovX bodies, and the Ang2 antibody 3.19.3 slowed the growth of colon and lung cancer xenografts and accentuated the activity of VEGF pathway inhibitors [10,15,16]. The dual Ang1/2 inhibitor, trebananib (AMG386), was found to have more activity than Ang2-specific inhibitors alone in colon cancer models [9]. Falcón et al. described similar findings in a colon cancer model and showed that Ang1 inhibition augmented the effect of Ang2 inhibition by preventing vascular normalization seen with the Ang2 inhibitor [13]. RCC is typified by Von Hippel–Lindau (VHL) loss leading to exquisite dependency on the VEGF-driven angiogenesis. As a consequence, RCC exposure to VEGF pathway inhibitors has been shown to result in "vascular infarction" rather than vascular normalization. Given this distinct biology, we sought to determine the relative effects on tumor growth and perfusion of Ang1, Ang2, and dual Ang1/2 inhibition alone and in combination with VEGF pathway inhibitors in a mouse model of RCC.

Another key question related directly to the clinical development of Ang inhibitors is how to select the patients most likely to benefit from this treatment. Currently, there is little data to guide optimal patient selection and determine the optimal treatment setting. To explore the possibility that Ang2 may be a useful surrogate or predictive marker of activity in RCC, we measured Ang2 plasma levels in patients with RCC either at presentation or during the course of VEGFR-targeted therapy. Taken together, these data inform the continued exploration of Ang2 inhibitors such as trebananib in patients with RCC or other cancers.

Materials and Methods

Evaluation of Gene Expression by Reverse Transcription–Polymerase Chain Reaction

Frozen tumor specimens of several human tumor types and non-malignant renal tissues, including non-malignant kidney tissue (cortex and medulla from non-oncology patients), clear cell RCC (ccRCC) tissue, and other non-renal tumor tissue including bladder, lymphoma, lung (adeno), lung (squamous), laryngeal, ovarian, prostate, gastric, breast, colorectal, and pancreatic tumors, were obtained. Total RNA was obtained either directly from a vendor (Ardais Corporation, Lexington, MA) or extracted from frozen tissue samples (Zoion Diagnostics Inc, Shrewsbury, MA) with the Qiagen RNeasy Mini Kit. All the RNA samples were treated with RNase-free DNase to remove genomic DNA before reverse transcription–polymerase chain reaction (RT-PCR). Quantitative RT-PCR was performed with 100 ng of total RNA in duplicate with a TaqMan EZ RT-PCR Kit from Roche (Indianapolis, IN). The primers and probes used in this study are listed in Table 1. *In vitro* transcripts of cDNA fragments for each gene were used as standard for calculating mRNA copy numbers. Cyclophilin A mRNA copy number was used for normalization.

Plasma Ang2 Measurement

Circulating Ang2 levels were measured in plasma collected from 50 patients with metastatic RCC, 39 patients with stage I RCC before nephrectomy, and 26 healthy volunteers. All 89 patients with RCC had histologically confirmed RCC (99% ccRCC, n = 88), and all provided written informed consent for sample collection. Samples were collected from healthy volunteers not being seen in any specialty clinics and who had no RCC pathology or urologic issues. Approval for the RCC sample collection protocol was obtained from the Institutional Review Board of the Dana-Farber/Harvard Cancer

Table 2. Characteristics of Patients Included in the Plasma Studies.

Patient Characteristics	Sunitinib (N = 44)	
Age	57 (Median)	41-76 (Range)
Gender	Number	Percentage
M	31	70.5
F	13	29.5
Previous nephrectomy	Number	Percentage
Y	39	88.6
N	5	11.4
Antiangiogenic drug	Number	Percentage
Sunitinib	42	95.5
Sorafenib	1	2.3
Pazopanib	1	2.3
Prior line(s) of treatment	Number	Percentage
1	12	27.3
2	16	36.4
3	11	25.0
4	4	9.1
5	0	0
6	1	2.3
Prior treatment	Number	Percentage
IL-2	20	45.5
Avastin	13	29.5
Sorafenib	12	27.3
Pazopanib	2	4.5
Axitinib	3	6.8
mTOR inhibitor**	2	4.5
Clinical trial	9	20.5
Other	4	9.1

* Of the 39 patients who had prior Nx, 24 had cytoreductive nephrectomy. All patients were treated with VEGFR TKI for metastatic disease and not in the adjuvant or neoadjuvant setting.

** Mammalian target of rapamycin.

Center (Boston, MA). Additionally, plasma from 44 patients with metastatic disease who were treated with sunitinib was collected. Characteristics for the metastatic RCC cohort are listed in Table 2. These patients received 50 mg of sunitinib daily for the first 4 weeks (~ 28 days) of 6-week cycles until disease progression was documented per response evaluation criteria in solid tumors criteria. Blood samples were collected in sodium citrate tubes at baseline, approximately 4 weeks into treatment (median day 34.5), and at the time of disease progression. Samples were centrifuged at 1500 rpm for 10 minutes within 60 minutes of collection. Plasma samples were stored at –80°C. Plasma Ang2 concentration was measured by ELISA (R&D Systems, Minneapolis, MN).

Cell Culture

A498, a VHL-deficient human RCC cell line, was obtained from the American Type Culture Collection (ATCC, Manassas, VA). Fresh frozen aliquots were used for each experiment. A498 cells were grown in Eagle's minimum essential medium. All media were supplemented with 2 mM L-glutamine, 10% fetal calf serum, and 1% streptomycin (50 μg/ml), and cells were cultured at 37°C with 5% CO_2.

Tumor Xenograft Induction

For subcutaneous xenograft tumor models, female athymic nude/beige mice (Charles River Laboratories, Wilmington, MA) were used. All experiments were approved by the Institutional Animal Care and Use Committee at Beth Israel Deaconess Medical Center. The mice were housed and maintained in laminar flow cabinets under specific pathogen-free conditions, and throughout the entirety of the study, all efforts were made to minimize suffering.

A498 cells were harvested from subconfluent cultures by a brief exposure to 0.25% trypsin and 0.02% EDTA. Trypsinization was stopped with medium containing 10% FBS, and the cells were washed once in serum-free medium and resuspended in phosphate-buffered saline as vehicle. Only suspensions consisting of single cells with greater than 90% viability were used for the injections.

To establish RCC tumor xenografts, A498 tumor cells were injected subcutaneously (1×10^7 cells) into the flanks of 6- to 8-week-old mice that were of 20 g average body weight. Tumors developed in >80% of mice and were usually visible within a few days of implantation. Once they reached a diameter of 3 to 5 mm, tumors were measured daily with calipers to ensure a consistent size at the outset of treatment. Treatment was initiated when the tumors had grown to a diameter of 12 mm as previously described [6]. For the single agent study, mice were randomized to the following treatment arms: Fc control, mL4-3, L1-7, trebananib. For the combination study, the arms were given as follows: Fc control, sunitinib, trebananib, trebananib + sunitinib, sunitinib + L1-7, and sunitinib + mL4-3. The dosing and schedule of treatment are given as follows: sunitinib (53.6 mg/kg) was administered 6 of 7 days per week by gavage. Human Fc (2.8 mg/kg, twice weekly), Ang1 inhibitor mL4-3 (20 mg/kg, daily), Ang2 inhibitor L1-7 (2.8 mg/kg, twice weekly), and dual Ang1/2 inhibitor (AMG 386, trebananib) (2.8 mg/kg, twice weekly) were injected subcutaneously. Tumor long axis and short axis were measured daily. Tumor volume was calculated by the

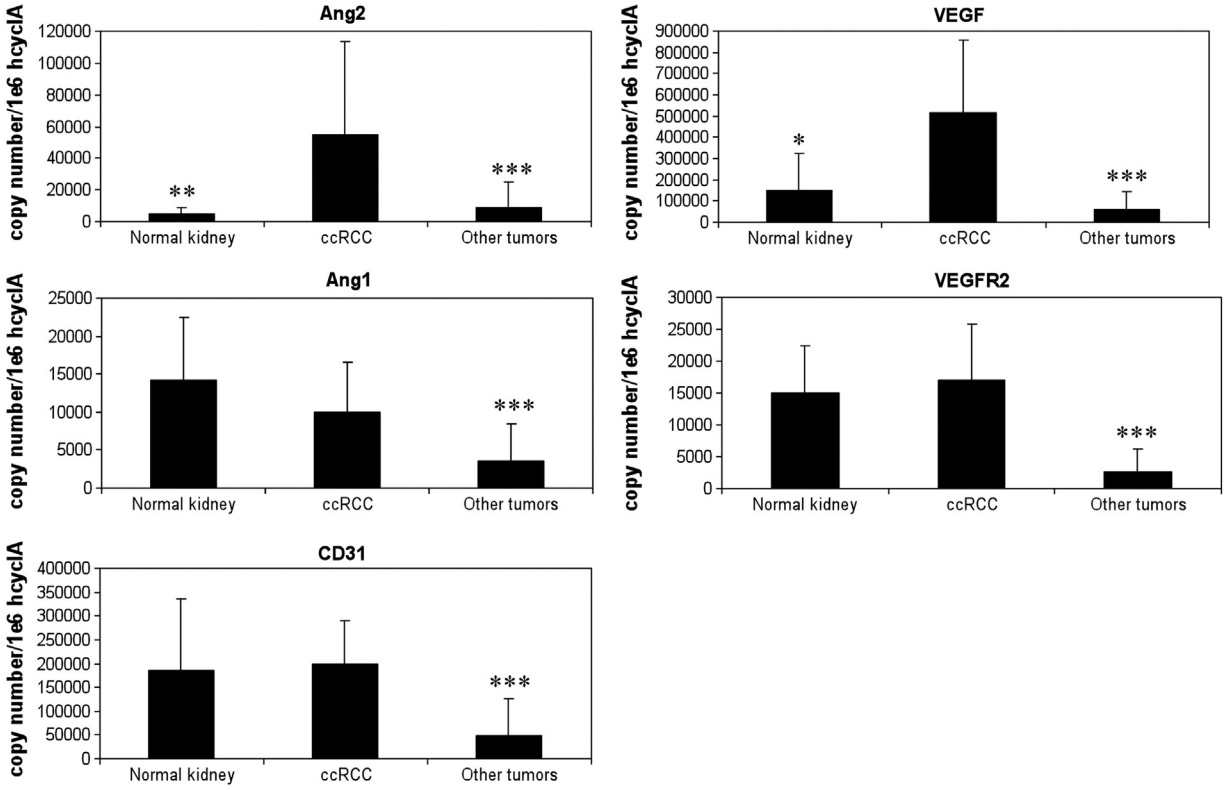

Figure 1. RT-PCR analysis of multiple tumor types shows that Ang2, VEGF, Ang1, VEGFR2, and CD31 are highly expressed in patients with ccRCC *versus* other tumor types (bladder, lymphoma, lung, laryngeal, ovarian, prostate, gastric, breast, colorectal, and pancreatic tumors). Ang2 and VEGF are also highly expressed in ccRCC *versus* normal kidney tissue. Data are expressed as means ± SD. *$P < 0.05$, **$P < 0.01$, ***$P < 0.001$.

formula long axis × short axis × short axis/2 to determine growth curves. Treatment was continued until tumors grew to 20 mm (i.e., the maximum allowable growth by Institutional Animal Care and Use Commitee) or roughly day 50, at which point the mice were killed.

Tumor Perfusion Imaging

Tumor perfusion imaging with arterial spin-labeled magnetic resonance imaging (ASL MRI) was performed as previously described [5,17,18] and quantified using standard methods [19]. A single transverse slice of ASL was carefully positioned at the center of the tumor, which was marked on the skin with a permanent marker pen for follow-up MRI studies. To determine tumor perfusion, a region of interest was drawn freehand around the peripheral margin of the tumor by using an electronic cursor on the reference image that was then copied to the perfusion image. The mean blood flow for the tumor tissue within the region of interest was derived.

Statistical Analysis

Statistical significance was calculated for the plasma analysis by Wilcoxon sign rank test for paired data and Wilcoxon rank sum for unpaired data. Tumor growth curves are presented with mean tumor volume ± standard error. Tumor perfusion comparisons were performed using a Student's *t*-test. $P < 0.05$ was considered significant.

Results

Ang2 Expression Is Elevated in Patients with RCC

Expression of *Ang2* and other angiogenic genes including *Ang1*, *VEGF*, *VEGFR2*, and *CD31* was analyzed by RT-PCR from samples of non-malignant kidney tissue ($n = 4$), ccRCC tissue ($n = 16$), and other non-renal tumor tissue including bladder, lymphoma, lung (adeno), lung (squamous), laryngeal, ovarian, prostate, gastric, breast, colorectal, and pancreatic tumors ($n = 133$; Figure 1). *Ang2* expression levels in ccRCC were 6.3-fold higher than in all other tumor types ($P < 0.001$). *Ang2* expression in ccRCC was 11.3-fold higher than in normal kidney tissue ($P = 0.0074$). *Ang1* expression levels in RCC and in other tumor types were lower than in normal kidney tissue ($P < 0.001$).

VEGF, *VEGFR2*, and *CD31* gene expression levels were all higher in ccRCC than in other tumors (8.4-fold for *VEGF*, $P < 0.001$; 6.3-fold for *VEGFR2*, $P < 0.001$; and 4.0-fold for *CD31*, $P < 0.001$; Figure 1). *VEGF* gene expression level was 3.4-fold higher in ccRCC than in normal kidney ($P = 0.0499$).

Plasma Ang2 Is Elevated in Patients with RCC

Plasma Ang2 was significantly higher in patients with metastatic RCC ($n = 50$; median 3720 pg/ml; range [1010, 29,006]) compared to plasma from healthy controls ($n = 26$; median 2255 pg/ml; [664, 6545]) and patients with stage I disease ($n = 39$; median 1394 pg/ml; [520, 7784]; $P < 0.001$; Figure 2*A*). Characteristics for the metastatic RCC cohort are shown in Table 2. Ang2 levels were also measured in patients at baseline, approximately day 29 (median day 34.5) after sunitinib initiation and at the time of disease progression on sunitinib. Plasma Ang2 levels decreased on sunitinib therapy ($n = 39$ pairs; median baseline 3387 pg/ml, range [1010, 14149], median on sunitinib (day 29) 1721 pg/ml; [325, 6584], $P < 0.01$) and increased from day 29 at the time of disease progression ($n = 28$ pairs; 2654.56 pg/ml; [1284, 10555]; $P < 0.01$; Figure 2*B*). Of the patients with baseline and day 29 samples, 5 of the 39 (13%) had dose modifications during this period and of the 28 patients in the day 29/progression group, 7 (25%) had dose modifications during the time they were on therapy.

Ang Inhibition Slows RCC Tumor Growth In Vivo

The effects of single agent mL4-3 (Ang1 inhibitor), L1-7 (Ang2 inhibitor), and trebananib (Ang1/2 inhibitor) were assessed on A498 RCC tumor growth. As single agents, trebananib and L1-7 slowed A498 RCC tumor growth compared to Fc control. mL4-3 showed little effect on A498 RCC tumor growth (Figure 3*A*).

To assess the impact of Ang inhibition on tumor perfusion, ASL MRI was performed on three or more tumors in each group at baseline, 1 and 3 weeks after treatment. A significant reduction in tumor perfusion was observed after trebananib or L1-7 treatment but not mL4-3 compared to Fc control group at day 7 (Fc: 142.9 ± 17.5 ml/100 g per min *vs* L1-7: 50.6 ± 23.6 ml/100 g per min, $P = 0.006$; *vs* trebananib: 60.2 ± 22.8 ml/100 g per min, $P = 0.008$; *vs* mL4-3: 113.1 ± 24.8 ml/100 g per min, $P = 0.204$) and day 21 (Fc: 88.4 ± 40.9 ml/100 g per min *vs* L1-7: 28.1 ± 7.3 ml/100 g per min, $P = 0.049$; *vs* trebananib: 37.8 ± 11.3 ml/100 g per min, $P = 0.029$; *vs* mL4-3: 68.4 ± 14.5 ml/100 g per min, $P = 0.566$; Figure 3, *B* (representative images) and *C*). This is consistent with previous reports that Ang2 blockade inhibits tumor angiogenesis in other tumor models [9,20].

Trebananib Potentiates the Antitumor Effects of Sunitinib on RCC Xenograft Tumor Growth and Perfusion

Sunitinib is an established treatment for patients with RCC; however, despite initial responses, resistance develops in all patients.

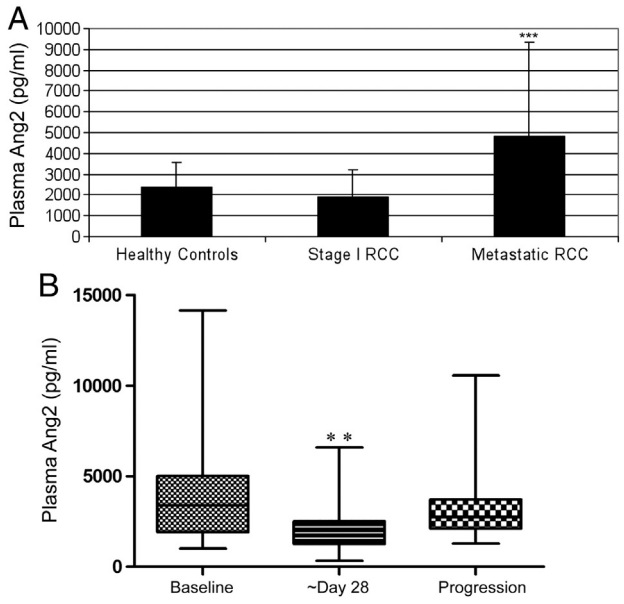

Figure 2. Analysis of Ang2 levels in patient plasma. (A) Patients with metastatic RCC have higher circulating plasma Ang2 levels than patients with (low burden) stage 1 RCC or healthy controls (***$P < 0.001$). (B) Plasma analysis in patients at baseline prior to treatment with sunitinib, ~day 28 after starting sunitinib, and at the time of progression on sunitinib shows that Ang2 levels decrease with sunitinib treatment and increase at the time of disease progression (**$P < 0.01$ for both comparisons). Data are expressed as means ± SD.

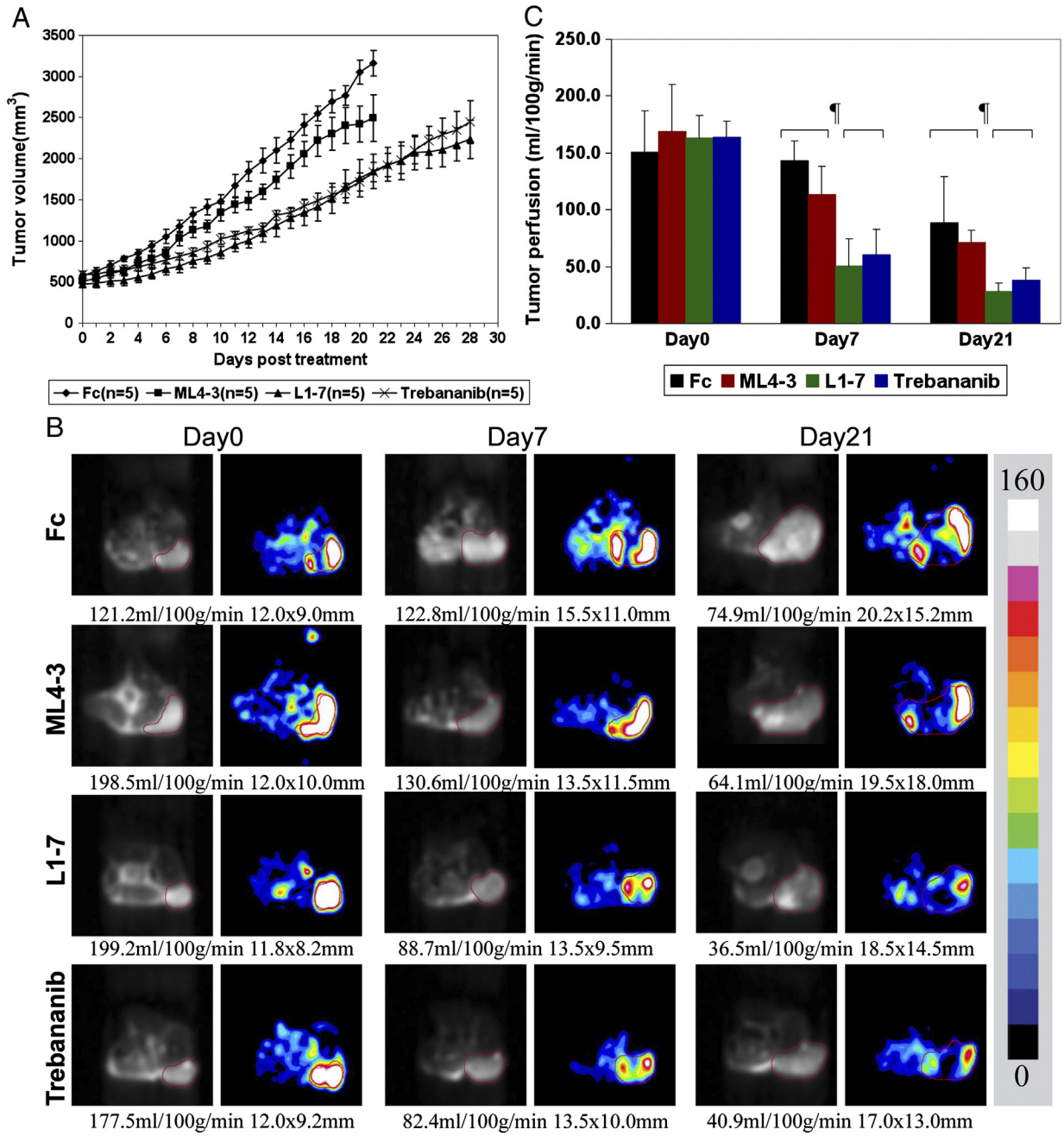

Figure 3. Single agent effect on A498 RCC xenograft tumor growth and perfusion. (A) This figure shows that trebananib (Ang1/2 inhibitor) and L1-7 (Ang2 inhibitor) slow A498 RCC tumor growth. Ang1 inhibition (mL4-3) did not alter A498 RCC tumor growth. (B, C) Representative ASL MRI images and quantitative tumor perfusion results in A498 RCC xenograft tumor model at days 0, 7, and 21 after treatment with trebananib (Ang1/2 inhibitor), L1-7 (Ang2 inhibitor), mL4-3 (Ang1 inhibitor), or Fc demonstrate significant reduction of tumor perfusion observed after Ang2 inhibition but not Ang1 inhibition alone compared with the Fc group at days 7 and 21 ($^{¶}P < 0.05$). Data are expressed as means ± SD. Tumor regions are outlined with a red line in reference proton density images and corresponding ASL perfusion color maps. The tumor size (mm) and the mean blood flow (in ml/100 g per min) are shown below the images. The color bar beside the images represents the range of perfusion values from 0 to 160 ml/100 g per min.

We assessed the effect of combining Ang1 and/or Ang2 inhibition and VEGFR inhibition with sunitinib (Figure 4). In the A498 tumor model, trebananib and L1-7 improved the antitumor activity of sunitinib to a similar extent (Figure 4A). However, mL4-3 did not enhance the tumor growth control of sunitinib.

To investigate the effects of sunitinib alone or in combination with trebananib, L1-7, or mL4-3 on tumor perfusion, ASL MRI was performed at baseline and 1, 3, and 7 weeks after treatment. The combination of sunitinib with either Ang2 inhibitor (trebananib or L1-7) prevented the resumption of perfusion seen in tumors treated with sunitinib alone at around day 50 after treatment (Figure 4, *B* (representative images) and *C*). Tumor perfusion in both the combination arms of sunitinib + trebananib or sunitinib + L1-7 was lower than in the sunitinib arm at day 50 (sunitinib + Fc: 36.7 ± 15.0 ml/100 g per min *vs* sunitinib + trebananib: 18.4 ± 11.1 ml/100 g per min; *vs* sunitinib + L1-7: 16.0 ± 7.3 ml/100 g per min, $P < 0.001$).

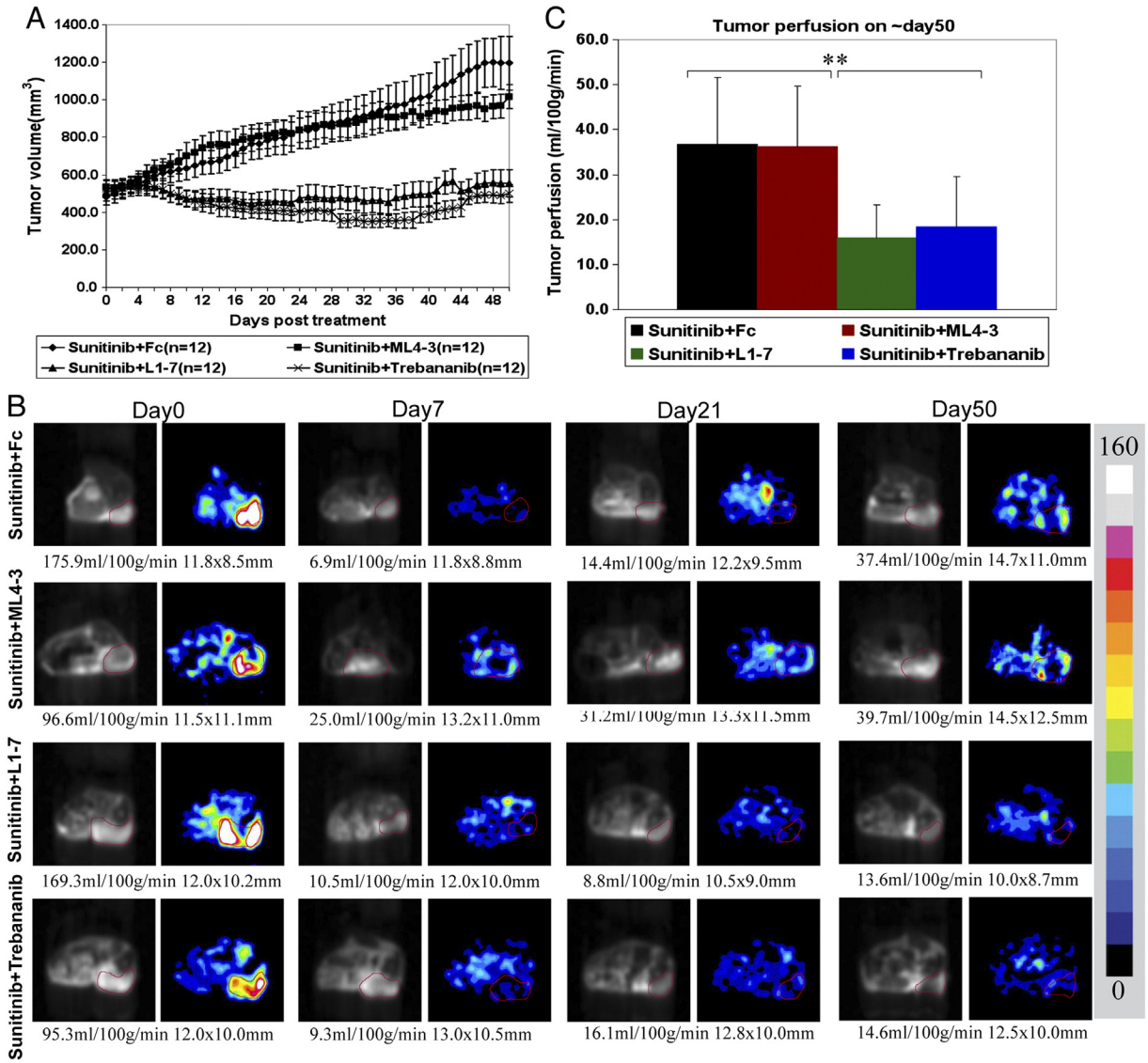

Figure 4. Combination studies of trebananib, L1-7, and mL4-3 with sunitinib on RCC xenograft tumor growth and perfusion. (A) Both trebananib and L1-7 improved the activity of sunitinib to a similar extent. mL4-3 did not improve sunitinib activity. (B) Representative ASL MRI perfusion images show tumor perfusion results at baseline (pretreatment), 1 week, 3 weeks, and 7 weeks after treatment with sunitinib + Fc, sunitinib + mL4-3, sunitinib + L1-7, and sunitinib + trebananib. Combination treatment of sunitinib and L1-7 or trebananib prevented or delayed the resumption of tumor perfusion compared to sunitinib + Fc treatment. Trebananib and L1-7 had similar effects on tumor perfusion reduction and prevention of tumor perfusion resumption with sunitinib treatment alone. Tumor regions are outlined in red in ASL perfusion images (right column of each time point) and the corresponding reference proton density images (left column). The tumor size (in mm) and mean blood flow (in ml/100 g per min) are shown below each image. The color bar beside the images represents the range of perfusion values from 0 to 160 ml/100 g per min. (C) Bar graph demonstrating the quantification of ASL MRI tumor perfusion at the time of resistance to sunitinib (~ day 50 after treatment). The combination of sunitinib and either trebananib or L1-7 prevented the restoration of tumor perfusion observed with sunitinib alone at the time of resistance (**$P < 0.001$).

This suggests the possibility that the addition of Ang2 inhibitors (but not single agent Ang1 inhibition) may suppress alternate angiogenic pathways active in the setting of VEGFR inhibition.

Discussion

We have studied several aspects of Ang2 biology as it relates to RCC. We showed that Ang2 is highly expressed in RCC *versus* other tumor types and that patients with metastatic RCC have high Ang2 levels that decrease with sunitinib treatment and frequently increase at the time of tumor resistance. We also showed in RCC mouse models that Ang2 inhibition combined with VEGFR inhibition slows tumor progression independent of Ang1 inhibition and that inhibition correlates with tumor blood flow as measured by MR-based perfusion imaging.

Our data suggest that the relative expression of Ang2 may vary across multiple tumor types. Given the activity of Ang2 inhibitors in RCC xenografts, it is tempting to hypothesize that the relative expression of Ang2 in a tumor might predict for sensitivity to Ang2 inhibition. This would further suggest that bladder cancer, being also a strong Ang2 expressor, would also be predicted to benefit from Ang2 inhibition. ccRCC also exhibited high levels of CD31, VEGFR2, and VEGF expression in addition to Ang2, possibly

contributing to the beneficial effect of combined sunitinib and Ang2 inhibition in delaying both disease progression and restoration of perfusion in RCC xenografts models. One limitation of this study is that we have not described the exact mechanism for the combinatorial effect on tumor perfusion. Further studies of the relationship of VEGF and Ang2 in tumor angiogenesis *in vivo* are needed. The necessity of VEGF pathway expression for sensitivity to Ang2 inhibitors either alone or in combination with VEGF inhibitors could also be investigated in other tumors such as bladder cancer.

In this study, we confirmed earlier findings that plasma Ang2 levels are increased in patients with RCC and that these levels decrease in patients with advanced RCC on treatment with sunitinib. Our results suggest that Ang2 may be a surrogate marker for angiogenic capacity of a tumor and may be a marker of endothelial burden. As endothelial cells are the target of VEGF blocking therapy, Ang2 levels may also correlate with the activity of VEGF pathway inhibitors. Larger studies are needed to explore these hypotheses.

We also showed that Ang2 levels increase at a time when RCC becomes resistant to sunitinib therapy. The hypothesis that Ang2 levels correlate with tumor angiogenic activity is further supported by the data that Ang2 levels increase in a majority of patients at the time of disease progression. Previous studies have shown that resistance to VEGFR TKI therapy is in part due to "angiogenic escape" or renewed angiogenesis that may be independent of VEGF [5,21]. We hypothesize that the rise in Ang2 seen at the time of disease resistance to VEGFR TKI therapy is a marker of resumed tumor angiogenesis. This raises the possibility that an Ang2 inhibitor might demonstrate activity in the setting of VEGFR TKI–resistant RCC. Not all patients exhibited elevated Ang2 at the time of disease progression, raising the possibility that increased Ang2 might predict for subsequent response to Ang inhibition. As Ang2 inhibitors are in the clinic, this hypothesis could be prospectively evaluated in clinical trials. Consistent with our previous studies, the current study demonstrated that ASL MRI has great practical potential as a non-invasive marker for monitoring tumor angiogenesis without introducing any extrinsic contrast agents [5,6,17,18]; others have shown that dynamic contrast-enhanced MRI may also be useful for monitoring therapy [22].

Trebananib is a dual Ang1/2 inhibitor that antagonizes Tie2 signaling by binding to and sequestering Ang1 and Ang2. Trebananib has been tested in several phase I and II clinical trials [23,24], and three phase III trials are ongoing in ovarian cancer (TRINOVA-1, TRINOVA-2, and TRINOVA-3). TRINOVA-1, evaluating trebananib plus paclitaxel *versus* placebo plus paclitaxel in recurrent ovarian cancer, was recently reported to have met its primary end point of progression-free survival (hazard ratio = 0.66, $P < 0.001$) [25].

Recent work suggests that Ang1 inhibition augments Ang2 inhibition in certain settings, but none of these studies were performed in models of RCC [9,13,20]. We found that in a VHL-deficient RCC model, Ang1/2 dual inhibition showed the same activity as the Ang2 alone inhibition. Thus, our data support the hypothesis that in RCC, either Ang2 or combined Ang1/Ang2 inhibition may be effective in combination with VEGFR inhibition in the clinical setting.

References

[1] Motzer RJ, Hutson TE, Tomczak P, Michaelson MD, Bukowski RM, Oudard S, Negrier S, Szczylik C, Pili R, and Bjarnason GA, et al (2009). Overall survival and updated results for sunitinib compared with interferon alfa in patients with metastatic renal cell carcinoma. *J Clin Oncol* **27**, 3584–3590.

[2] Escudier B, Eisen T, Stadler WM, Szczylik C, Oudard S, Staehler M, Negrier S, Chevreau C, Desai AA, and Rolland F, et al (2009). Sorafenib for treatment of renal cell carcinoma: final efficacy and safety results of the phase III treatment approaches in renal cancer global evaluation trial. *J Clin Oncol* **27**, 3312–3318.

[3] Sternberg CN, Davis ID, Mardiak J, Szczylik C, Lee E, Wagstaff J, Barrios CH, Salman P, Gladkov OA, and Kavina A, et al (2010). Pazopanib in locally advanced or metastatic renal cell carcinoma: results of a randomized phase III trial. *J Clin Oncol* **28**, 1061–1068.

[4] Rini BI, Escudier B, Tomczak P, Kaprin A, Szczylik C, Hutson TE, Michaelson MD, Gorbunova VA, Gore ME, and Rusakov IG, et al (2011). Comparative effectiveness of axitinib versus sorafenib in advanced renal cell carcinoma (AXIS): a randomised phase 3 trial. *Lancet* **378**, 1931–1939.

[5] Schor-Bardach R, Alsop DC, Pedrosa I, Solazzo SA, Wang X, Marquis RP, Atkins MB, Regan M, Signoretti S, and Lenkinski RE, et al (2009). Does arterial spin-labeling MR imaging-measured tumor perfusion correlate with renal cell cancer response to antiangiogenic therapy in a mouse model? *Radiology* **251**, 731–742.

[6] Bhatt RS, Wang X, Zhang L, Collins MP, Signoretti S, Alsop DC, Goldberg SN, Atkins MB, and Mier JW (2010). Renal cancer resistance to antiangiogenic therapy is delayed by restoration of angiostatic signaling. *Mol Cancer Ther* **9**, 2793–2802.

[7] Huang D, Ding Y, Zhou M, Rini BI, Petillo D, Qian CN, Kahnoski R, Futreal PA, Furge KA, and Teh BT (2010). Interleukin-8 mediates resistance to antiangiogenic agent sunitinib in renal cell carcinoma. *Cancer Res* **70**, 1063–1071.

[8] Casanovas O, Hicklin DJ, Bergers G, and Hanahan D (2005). Drug resistance by evasion of antiangiogenic targeting of VEGF signaling in late-stage pancreatic islet tumors. *Cancer Cell* **8**, 299–309.

[9] Coxon A, Bready J, Min H, Kaufman S, Leal J, Yu D, Lee TA, Sun JR, Estrada J, and Bolon B, et al (2010). Context-dependent role of angiopoietin-1 inhibition in the suppression of angiogenesis and tumor growth: implications for AMG 386, an angiopoietin-1/2-neutralizing peptibody. *Mol Cancer Ther* **9**, 2641–2651.

[10] Huang H, Lai JY, Do J, Liu D, Li L, Del Rosario J, Doppalapudi VR, Pirie-Shepherd S, Levin N, and Bradshaw C, et al (2011). Specifically targeting angiopoietin-2 inhibits angiogenesis, Tie2-expressing monocyte infiltration, and tumor growth. *Clin Cancer Res* **17**, 1001–1011.

[11] Herbst RS, Hong D, Chap L, Kurzrock R, Jackson E, Silverman JM, Rasmussen E, Sun YN, Zhong D, and Hwang YC, et al (2009). Safety, pharmacokinetics, and antitumor activity of AMG 386, a selective angiopoietin inhibitor, in adult patients with advanced solid tumors. *J Clin Oncol* **27**, 3557–3565.

[12] Karlan BY, Oza AM, Richardson GE, Provencher DM, Hansen VL, Buck M, Chambers SK, Ghatage P, Pippitt Jr CH, and Brown 3rd JV, et al (2012). Randomized, double-blind, placebo-controlled phase II study of AMG 386 combined with weekly paclitaxel in patients with recurrent ovarian cancer. *J Clin Oncol* **30**, 362–371.

[13] Falcón BL, Hashizume H, Koumoutsakos P, Chou J, Bready JV, Coxon A, Oliner JD, and McDonald DM (2009). Contrasting actions of selective inhibitors of angiopoietin-1 and angiopoietin-2 on the normalization of tumor blood vessels. *Am J Pathol* **175**, 2159–2170.

[14] Gerald D, Chintharlapalli S, Augustin HG, and Benjamin LE (2013). Angiopoietin-2: an attractive target for improved antiangiogenic tumor therapy. *Cancer Res* **73**, 1649–1657.

[15] Hashizume H, Falcón BL, Kuroda T, Baluk P, Coxon A, Yu D, Bready JV, Oliner JD, and McDonald DM (2010). Complementary actions of inhibitors of angiopoietin-2 and VEGF on tumor angiogenesis and growth. *Cancer Res* **70**, 2213–2223.

[16] Brown JL, Cao ZA, Pinzon-Ortiz M, Kendrew J, Reimer C, Wen S, Zhou JQ, Tabrizi M, Emery S, and McDermott B, et al (2010). A human monoclonal anti-ANG2 antibody leads to broad antitumor activity in combination with VEGF inhibitors and chemotherapy agents in preclinical models. *Mol Cancer Ther* **9**, 145–156.

[17] Zhang L, Bhasin M, Schor-Bardach R, Wang X, Collins MP, Panka D, Putheti P, Signoretti S, Alsop DC, and Libermann T, et al (2011). Resistance of renal cell carcinoma to sorafenib is mediated by potentially reversible gene expression. *PLoS One* **6**, e19144.

[18] Wang X, Zhang L, O'Neill A, Bahamon B, Alsop DC, Mier JW, Goldberg SN, Signoretti S, Atkins MB, and Wood CG, et al (2013). Cox-2 inhibition enhances the activity of sunitinib in human renal cell carcinoma xenografts. *Br J Cancer* **108**, 319–326.

[19] Alsop DC and Detre JA (1996). Reduced transit-time sensitivity in noninvasive magnetic resonance imaging of human cerebral blood flow. *J Cereb Blood Flow Metab* **16**, 1236–1249.

[20] Daly C, Eichten A, Castanaro C, Pasnikowski E, Adler A, Lalani AS, Papadopoulos N, Kyle AH, Minchinton AI, and Yancopoulos GD, et al (2013). Angiopoietin-2 functions as a Tie2 agonist in tumor models, where it limits the effects of VEGF inhibition. *Cancer Res* **73**, 108–118.

[21] Bergers G and Hanahan D (2008). Modes of resistance to anti-angiogenic therapy. *Nat Rev Cancer* **8**, 592–603.

[22] Hillman GG, Singh-Gupta V, Al-Bashir AK, Zhang H, Yunker CK, Patel AD, Sethi S, Abrams J, and Haacke EM (2010). Dynamic contrast-enhanced magnetic resonance imaging of sunitinib-induced vascular changes to schedule chemotherapy in renal cell carcinoma xenograft tumors. *Transl Oncol* **3**, 293–306.

[23] Peeters M, Strickland AH, Lichinitser M, Suresh AV, Manikhas G, Shapiro J, Rogowski W, Huang X, Wu B, and Warner D, et al (2013). A randomised, double-blind, placebo-controlled phase 2 study of trebananib (AMG 386) in combination with FOLFIRI in patients with previously treated metastatic colorectal carcinoma. *Br J Cancer* **108**, 503–511.

[24] Eatock MM, Tebbutt NC, Bampton CL, Strickland AH, Valladares-Ayerbes M, Swieboda-Sadlej A, Van Cutsem E, Nanayakkara N, Sun YN, and Zhong ZD, et al (2013). Phase II randomized, double-blind, placebo-controlled study of AMG 386 (trebananib) in combination with cisplatin and capecitabine in patients with metastatic gastro-oesophageal cancer. *Ann Oncol* **24**, 710–718.

[25] http://wwwext.amgen.com/media/media_pr_detail.jsp?year=2013&releaseID=1829205.